

Irrotational Faraday Waves on a Viscous Fluid

T.Funada,* J.Wang,† D.D.Joseph,†‡ & N.Tashiro*

*Department of Digital Engineering, Numazu National College of Technology, 3600 Ooka, Numazu, Shizuoka, 410-8501, Japan

†Department of Aerospace Engineering and Mechanics, University of Minnesota, 110 Union St. SE, Minneapolis, MN 55455, USA

Abstract

An analysis of irrotational Faraday waves on an inviscid fluid was given by Benjamin and Ursell 1954. Here we extend the analysis of the same problem to purely irrotational waves on a viscous fluid. Following our earlier work on free surface problems, two irrotational theories are presented. In the first theory (VPF) the effects of viscosity enter only through the viscous normal stress term evaluated on the potential. In the second irrotational theory (VCVPF), a viscous contribution is added to the Bernoulli pressure; otherwise the second theory is the same as the first. The second theory VCVPF gives rise to the same damped Mathieu equation as the dissipation method. Pressure fields are not required and not used in the dissipation method. The dissipation method is a purely irrotational theory, though it depends on viscosity, in which only irrotational velocity fields $\mathbf{u} = \nabla\phi$ are needed. The two purely irrotational theories VPF and VCVPF are not restricted to small viscosities; they are restricted to small vorticity and do not apply near no-slip wall where vorticity is generated.

Our VCVPF and dissipation theories give the same damped Mathieu equation as the phenomenological approximation of Kumar and Tuckerman 1994. The damping term in VCVPF is twice the damping rate of VPF. The growth rates of unstable disturbances computed by VPF are uniformly larger than those computed by VCVPF (or equivalently by Kumar and Tuckerman). Comparisons with the exact solution and the Rayleigh-Taylor instability show that thresholds and growth rates for viscously damped waves are better described by VPF than VCVPF.

Contents

1	Introduction	2
2	Energy equation	2
3	VPF & VCVPF	3
3.1	Potential flow	3
3.2	Amplitude equations for the elevation of the free surface	4
4	Dissipation method	7
5	Stability analysis	9
5.1	Comparison of VPF and VCVPF for periodic waves in a deep liquid	10
5.2	Damped Mathieu equation; Experiments of Benjamin & Ursell	14
6	Rayleigh-Taylor instability and Faraday waves	18
7	Comparison of purely irrotational solutions with exact solutions	22
8	Conclusion	24

‡Author to whom correspondence should be addressed. Telephone: (612) 625-0309; fax (612) 626-1558; electronic mail: joseph@aem.umn.edu

1 Introduction

The seminal paper of Benjamin & Ursell (1954) (referred to as BU hereafter) on the stability of the plane free surface of a liquid in vertical periodic motion has spawned a huge literature which extends their analysis to include effects of viscosity, two liquids, side wall, bottom and free surface boundary layers and nonlinear effects associated with bifurcation and pattern formation. Review papers emphasizing different aspects of this problem have been prepared by Miles & Henderson (1990), Dias & Kharif (1999), and Perlin & Schultz (2000). This paper focuses on the effects of viscosity using viscous potential flow for exactly the same problem, in exactly the same formulation as Benjamin & Ursell (1954).

The flow literature on Faraday waves is not widely relevant to our problem except as to point to the effects which we do not consider. These neglected effects are the ones generated by no-slip boundary conditions at the bottom and side walls and all nonlinear effects. We have derived the following two damped Mathieu equations from systematic analysis of the irrotational motion of viscous fluids in the formulation and using the notations introduced by BU. Thus

$$\ddot{a}_m + N\nu\dot{a}_m k_m^2 + k_m \tanh(k_m h) \left[\frac{\gamma}{\rho} k_m^2 + (g - f \cos(\omega t)) \right] a_m = 0 \quad (1.1)$$

where k_m is an eigenvalue of the vibrating membrane equation

$$\frac{\partial^2 S_m}{\partial x^2} + \frac{\partial^2 S_m}{\partial y^2} + k_m^2 S_m = 0 \quad (1.2)$$

and

$$N = 2 \text{ (VPF)}, \quad N = 4 \text{ (VCVPF)}.$$

The damped equation (1.1) with $N = 4$ was presented as a phenomenological model using a damping coefficient given by Landau & Lifshitz (1987) (§25) by Kumar & Tuckerman (1994). Their *ad hoc* equation is advertised as valid for small damping. Here we obtain the equations with $N = 2$ and $N = 4$ from systematic analysis of the equations which govern the irrotational flows of viscous fluids. No restrictions on the values of ν arise in the analysis and we argue that equations are valid for large as well as small damping. Moreover, we find that the damped Mathieu equation (1.1) with $N = 2$ gives a better approximation to small amplitude Faraday dynamics than $N = 4$ for which the waves are “overdamped.”

Our analysis includes many tables and graphs which are rapidly, easily and accurately computed by a Runge-Kutta (RK) integration of the initial value problems associated with (1.1) (see Funada *et al.* (2005)).

2 Energy equation

The energy equation is the basis of our VCVPF theory. We derive the mechanical energy equation from Navier-Stokes equations

$$\rho \frac{d\mathbf{u}}{dt} = \nabla \cdot \mathbf{T} + \rho(g - f \cos(\omega t)) \mathbf{e}_z \quad (2.1)$$

in the usual way; scalar multiply (2.1) by \mathbf{u} , integrate over the fluid domain V , apply Reynolds' transport theorem and Gauss' theorem, to find

$$\frac{d}{dt} \int_V \frac{1}{2} \rho |\mathbf{u}|^2 dV = \int_{A_f} \mathbf{u} \cdot \mathbf{T} \cdot \mathbf{n} dA + \int_{A_w} \mathbf{u} \cdot \mathbf{T} \cdot \mathbf{n} dA - \int_V 2\mu \mathbf{D} : \mathbf{D} dV + (g - f \cos(\omega t)) \int_V \rho \frac{dz}{dt} dV, \quad (2.2)$$

where A_f is the free surface, A_w represents both the side walls and the bottom wall, and \mathbf{n} is the outward normal of V on A . The integrals $\int_{A_f} \mathbf{u} \cdot \mathbf{T} \cdot \mathbf{n} dA$ and $\int_{A_w} \mathbf{u} \cdot \mathbf{T} \cdot \mathbf{n} dA$ are the power of traction. On the free surface $\mathbf{n} \approx -\mathbf{e}_z$ and we can show readily that

$$\mathbf{u} \cdot \mathbf{T} \cdot \mathbf{n} = -(u_x T_{xz} + u_y T_{yz} + u_z T_{zz}). \quad (2.3)$$

We shall be considering the potential flow of viscous fluids called VPF. For these flows, the no-slip conditions usually cannot be satisfied and they are replaced with (3.1) below. The stresses on the free surface are evaluated using potential flow

$$\left. \begin{aligned} T_{xz} = \tau_{xz}^i &= \mu \left(\frac{\partial u_x}{\partial z} + \frac{\partial u_z}{\partial x} \right), \\ T_{yz} = \tau_{yz}^i &= \mu \left(\frac{\partial u_y}{\partial z} + \frac{\partial u_z}{\partial y} \right), \\ T_{zz} = -p_i + \tau_{zz}^i &= -p_i + 2\mu \frac{\partial u_z}{\partial z}, \end{aligned} \right\} \quad (2.4)$$

where p_i is the irrotational pressure computed from the Bernoulli equation. Then the mechanical energy equation for VPF may be written as

$$\begin{aligned} \frac{d}{dt} \int_V \frac{1}{2} \rho |\mathbf{u}|^2 dV &= \int_{A_f} - [u_x \tau_{xz}^i + u_y \tau_{yz}^i + u_z (-p_i + \tau_{zz}^i)] dA + \int_{A_w} \mathbf{u} \cdot \mathbf{T} \cdot \mathbf{n} dA \\ &- \int_V 2\mu \mathbf{D} : \mathbf{D} dV + (g - f \cos(\omega t)) \int_V \rho \frac{dz}{dt} dV. \end{aligned} \quad (2.5)$$

The shear stresses τ_{xz}^i and τ_{yz}^i from the potential flow are not zero at the free surface. However, the shear stresses should be zero physically. T_{xz} and T_{yz} cannot be made zero in irrotational flows, but we can remove the power by the shear stress $\int_{A_f} (u_x \tau_{xz}^i + u_y \tau_{yz}^i) dA$ from the mechanical energy equation. At the same time, a pressure correction p_v is added to p_i to compensate for the shear stresses. The mechanical energy equation for VCVPF is then written as

$$\begin{aligned} \frac{d}{dt} \int_V \frac{1}{2} \rho |\mathbf{u}|^2 dV &= \int_{A_f} - [u_z (-p_i - p_v + \tau_{zz}^i)] dA + \int_{A_w} \mathbf{u} \cdot \mathbf{T} \cdot \mathbf{n} dA \\ &- \int_V 2\mu \mathbf{D} : \mathbf{D} dV + (g - f \cos(\omega t)) \int_V \rho \frac{dz}{dt} dV. \end{aligned} \quad (2.6)$$

A comparison of (2.5) and (2.6) gives rise to the relation between the pressure correction and the irrotational shear stresses

$$\int_{A_f} [u_x \tau_{xz}^i + u_y \tau_{yz}^i] dA = \int_{A_f} (-p_v u_z) dA. \quad (2.7)$$

3 VPF & VCVPF

There are two approaches to the analysis of the effects of viscosity in purely irrotational motions of real fluids. The first and simplest approach is to include the effects of the viscous normal stress in the normal stress balance; nothing more. The second approach is the same as the first except that an additional viscous pressure is computed to remove the effects of irrotational shear from the energy balance. We call this second approach VCVPF (viscous correction of viscous potential flow); it is equivalent to the well known dissipation method in which no pressure, viscous or inviscid, is required. The two theories VPF and VCVPF give rise to different results. Our experience with other problems is such as to suggest that VCVPF is closer to exact results for progressive waves, and VPF is closer to exact results when waves do not propagate, more precisely, in this case the eigenvalues are real. This second case, in which VPF is better, applies here to irrotational Faraday waves on viscous fluids.

3.1 Potential flow

The velocity $\mathbf{u} = \nabla \phi = (u_x, u_y, u_z)$ is expressed in terms of a harmonic potential $\nabla^2 \phi = 0$ in a coordinate system moving with the container. Boundary conditions at the container walls are given by

$$\left. \begin{aligned} \frac{\partial \phi}{\partial n} &= 0 \quad \text{on the side walls,} \\ \frac{\partial \phi}{\partial z} &= 0 \quad \text{on the bottom wall at } z = h. \end{aligned} \right\} \quad (3.1)$$

A harmonic solution satisfying (3.1) can be written as

$$\phi(x, y, z, t) = \sum_{m=0}^{\infty} f_m(t) \cosh [k_m (h - z)] S_m(x, y), \quad (3.2)$$

where the eigenfunctions $S_m(x, y)$ satisfy

$$\frac{\partial S_m}{\partial n} = 0, \quad (3.3)$$

on the side wall. The condition at the bottom wall gives

$$\left(\frac{\partial \phi}{\partial z} \right)_{z=h} = \sum_{m=0}^{\infty} f_m(t) (-k_m) \sinh [k_m (h - z)] S_m(x, y) \Big|_{z=h} = 0. \quad (3.4)$$

The normal stress balance at the free surface

$$z = \zeta(x, y, t), \quad (3.5)$$

in the linearized approximation, is

$$\left(p - 2\mu \frac{\partial u_z}{\partial z} \right)_{z=0} = \gamma \left(\frac{\partial^2 \zeta}{\partial x^2} + \frac{\partial^2 \zeta}{\partial y^2} \right). \quad (3.6)$$

For VPF, $p = p_i$ where p_i is given by the Bernoulli equation. For VCVPF, $p = p_i + p_v$ where p_v is a viscous correction of the irrotational pressure p_i .

3.2 Amplitude equations for the elevation of the free surface

Now consider the kinematic condition at $z = 0$

$$\frac{\partial \zeta}{\partial t} = u_z = \frac{\partial \phi}{\partial z} \quad \text{at } z = 0 \quad (3.7)$$

where

$$\left(\frac{\partial \phi}{\partial z} \right)_{z=0} = \sum_{m=0}^{\infty} f_m(t) (-k_m) \sinh (k_m h) S_m(x, y). \quad (3.8)$$

If we write the surface elevation as

$$\zeta = \sum_{m=0}^{\infty} a_m(t) S_m(x, y), \quad (3.9)$$

then

$$\frac{\partial \zeta}{\partial t} = \sum_{m=0}^{\infty} \frac{da_m}{dt} S_m(x, y). \quad (3.10)$$

Since the total volume of fluid is constant, $a_0(t)$ is constant

$$\frac{da_0}{dt} = 0$$

and

$$\frac{\gamma}{\rho} \left(\frac{\partial^2 \zeta}{\partial x^2} + \frac{\partial^2 \zeta}{\partial y^2} \right) = -\frac{\gamma}{\rho} \sum_{m=1}^{\infty} k_m^2 a_m(t) S_m(x, y). \quad (3.11)$$

Since $k_0 = 0$, (3.11) and (3.8) show that $f_0(t)$ is undetermined. BU showed that $a_0(t)$ can be put to zero.

For $m \geq 1$, (3.7), (3.8) and (3.10) give

$$\frac{da_m}{dt} S_m(x, y) = f_m(t) (-k_m) \sinh(k_m h) S_m(x, y), \quad \text{hence } f_m(t) = -\frac{da_m}{dt} \frac{1}{k_m \sinh(k_m h)},$$

so that the potential is given by

$$\phi(x, y, z, t) = -\sum_{m=1}^{\infty} \frac{da_m}{dt} \frac{\cosh[k_m(h-z)]}{k_m \sinh(k_m h)} S_m(x, y). \quad (3.12)$$

The Bernoulli's equation is

$$\frac{p_i}{\rho} + \frac{\partial \phi}{\partial t} - (g - f \cos(\omega t)) z = 0. \quad (3.13)$$

The normal stress balance (3.6) is

$$\left(p_i + p_v - 2\mu \frac{\partial u_z}{\partial z} \right)_{z=0} = \gamma \left(\frac{\partial^2 \zeta}{\partial x^2} + \frac{\partial^2 \zeta}{\partial y^2} \right). \quad (3.14)$$

Linearized governing equations for the viscous corrections are

$$\rho \frac{\partial \mathbf{u}_v}{\partial t} = -\nabla p_v + \mu \nabla^2 \mathbf{u}_v, \quad \nabla \cdot \mathbf{u}_v = 0. \quad (3.15)$$

Hence,

$$\nabla^2 p_v = 0. \quad (3.16)$$

The solution of (3.16) may be written as

$$-p_v = \sum_{m=0}^{\infty} C_m \hat{r}_m(t) \theta_m(z) S_m(x, y), \quad \theta_m = c_{m1} e^{k_m z} + c_{m2} e^{-k_m z}. \quad (3.17)$$

At $z = 0$,

$$-p_v(z = 0) = \sum_{m=0}^{\infty} C_m r_m(t) S_m(x, y), \quad (3.18)$$

where $r_m = \hat{r}_m(t) (c_{m1} + c_{m2})$.

We may eliminate p_i from (3.14) using (3.13)

$$\left[p_v + \rho (g - f \cos(\omega t)) \zeta - \rho \frac{\partial \phi}{\partial t} - 2\mu \frac{\partial^2 \phi}{\partial z^2} \right]_{x=0} = \gamma \left(\frac{\partial^2 \zeta}{\partial x^2} + \frac{\partial^2 \zeta}{\partial y^2} \right). \quad (3.19)$$

Equation (3.19) may be evaluated on modal functions using (3.9), (3.11),

$$2\mu \frac{\partial^2 \phi}{\partial z^2} = -2\mu \sum_{m=1}^{\infty} \frac{da_m}{dt} k_m \frac{\cosh[k_m(h-z)]}{\sinh(k_m h)} S_m(x, y) \quad (3.20)$$

and

$$\frac{\partial \phi}{\partial t} = -\sum_{m=1}^{\infty} \frac{d^2 a_m}{dt^2} \frac{\coth[k_m(h-z)]}{k_m \sinh(k_m h)} S_m(x, y). \quad (3.21)$$

Hence

$$\sum_{m=1}^{\infty} \left[-C_m r_m(t) + \rho(g - f \cos(\omega t)) a_m(t) + \rho \frac{d^2 a_m}{dt^2} \frac{\coth(k_m h)}{k_m} + 2\mu \frac{da_m}{dt} k_m \coth(k_m h) + \gamma k_m^2 a_m(t) \right] S_m(x, y) = 0. \quad (3.22)$$

The coefficients of the linearly independent functions $S_m(x, y)$ vanish. Hence the amplitude equation for VCVPF is

$$\frac{d^2 a_m}{dt^2} + 2\nu k_m^2 \frac{da_m}{dt} + k_m \tanh(k_m h) \left[\frac{\gamma}{\rho} k_m^2 + g - f \cos(\omega t) \right] a_m - \frac{k_m}{\rho} \tanh(k_m h) C_m r_m(t) = 0. \quad (3.23)$$

To evaluate $C_m r_m(t)$ in (3.23) we need to work only with mode m . To simplify the writing we shall suppress the subscript m and write

$$u_x = -\frac{da}{dt} \frac{\coth(kh)}{k} \frac{\partial S}{\partial x}, \quad (3.24)$$

$$\tau_{xz} = 2\mu \frac{da}{dt} \frac{\partial S}{\partial x}, \quad (3.25)$$

$$u_y = -\frac{da}{dt} \frac{\coth(kh)}{k} \frac{\partial S}{\partial y}, \quad (3.26)$$

$$\tau_{yz} = 2\mu \frac{da}{dt} \frac{\partial S}{\partial y}, \quad (3.27)$$

$$u_z = \frac{da}{dt} S, \quad (3.28)$$

$$p_v = -Cr(t)S, \quad (3.29)$$

$$\tau_{zz} = -2\mu \frac{da}{dt} k \coth(kh) S, \quad (3.30)$$

$$\int_A [u_x \tau_{xz} + u_y \tau_{yz} + p_v u_z] dA = \int_A \left\{ -2\mu \left(\frac{da}{dt} \right)^2 \frac{\coth(kh)}{k} \left[\left(\frac{\partial S}{\partial x} \right)^2 + \left(\frac{\partial S}{\partial y} \right)^2 \right] - Cr(t) \frac{da}{dt} S^2 \right\} dA = 0.$$

Using Gauss' theorem and the boundary condition on the side wall (3.3), we obtain

$$\int_A \left[\frac{\partial}{\partial x} \left(S \frac{\partial S}{\partial x} \right) + \frac{\partial}{\partial y} \left(S \frac{\partial S}{\partial y} \right) \right] dA = \int_L \left[S \frac{\partial S}{\partial n} \right] dL = 0,$$

where L is the boundary of the free surface A and L is on the side wall. With the condition $\nabla_2^2 S = -k^2 S$, we can show that

$$\int_A \left[\left(\frac{\partial S}{\partial x} \right)^2 + \left(\frac{\partial S}{\partial y} \right)^2 \right] dA = - \int_A S \nabla_2^2 S dA = k^2 \int_A S^2 dA. \quad (3.31)$$

We find that

$$\left(2\mu \left(\frac{da}{dt} \right)^2 k \coth(kh) + Cr(t) \frac{da}{dt} \right) \int S^2 dA = 0 \quad (3.32)$$

and

$$C_m r_m(t) = Cr(t) = -2\mu k \frac{da}{dt} \coth(kh). \quad (3.33)$$

Inserting (3.33) into (3.23) we find the amplitude equation for VCVPF

$$\frac{d^2 a}{dt^2} + 4\nu k^2 \frac{da}{dt} + k \tanh(kh) \left[\frac{\gamma}{\rho} k^2 + g - f \cos(\omega t) \right] a = 0. \quad (3.34)$$

Viscous potential flow VPF is the same as VCVPF without the pressure correction p_v . If p_v is set to zero, we find that

$$\frac{d^2 a}{dt^2} + 2\nu k^2 \frac{da}{dt} + k \tanh(kh) \left[\frac{\gamma}{\rho} k^2 + g - f \cos(\omega t) \right] a = 0. \quad (3.35)$$

The damping term can be written as

$$N\nu k^2 \frac{da}{dt} \quad (3.36)$$

with $N = 2$ for VPF and $N = 4$ for VCVPF.

4 Dissipation method

We now show that the dissipation method leads to the same amplitude equation (3.34) which we derived for VCVPF. The two theories are equivalent, but no pressure, whatever is required to implement the dissipation method. To show this, we evaluate (2.2), term by term. Thus

$$\phi = -\frac{da}{dt} \frac{\cosh[k(h-z)]}{k \sinh(kh)} S(x, y), \quad (4.1)$$

$$|\mathbf{u}|^2 = |\nabla\phi|^2 = \left(\frac{da}{dt} \right)^2 \frac{1}{\sinh^2(kh)} \left[\frac{1}{2} \cosh(2k(h-z)) \left(\frac{|\nabla_2 S|^2}{k^2} + S^2 \right) + \frac{1}{2} \left(\frac{|\nabla_2 S|^2}{k^2} - S^2 \right) \right].$$

Using (3.31), we find that

$$\int_V |\mathbf{u}|^2 dV = \int_0^h \int |\mathbf{u}|^2 dAdz = \int_0^h \left(\frac{da}{dt} \right)^2 \frac{\cosh(2k(h-z))}{\sinh^2(kh)} dz \int S^2 dA = \left(\frac{da}{dt} \right)^2 \frac{\coth(kh)}{k} \int S^2 dA.$$

Hence

$$\frac{d}{dt} \int_V \frac{1}{2} \rho |\mathbf{u}|^2 dV = \rho \frac{da}{dt} \frac{d^2 a}{dt^2} \frac{\coth(kh)}{k} \int S^2 dA. \quad (4.2)$$

We next consider the power of traction $\int_{A_f} \mathbf{u} \cdot \mathbf{T} \cdot \mathbf{n} dA + \int_{A_w} \mathbf{u} \cdot \mathbf{T} \cdot \mathbf{n} dA$. On the free surface $\mathbf{n} \approx -\mathbf{e}_z$ and we have already derived that

$$\mathbf{u} \cdot \mathbf{T} \cdot \mathbf{n} = -(u_x T_{xz} + u_y T_{yz} + u_z T_{zz}).$$

The physical boundary conditions require that

$$T_{xz} = 0, \quad T_{yz} = 0, \quad T_{zz} = -\gamma \left(\frac{\partial^2 \zeta}{\partial x^2} + \frac{\partial^2 \zeta}{\partial y^2} \right),$$

where $u_z = da/dt S(x, y)$ at the free surface and $\zeta = a(t)S(x, y)$ and

$$\frac{\gamma}{\rho} |\nabla_2 S|^2 = \frac{\gamma}{\rho} \left(\frac{\partial^2 \zeta}{\partial x^2} + \frac{\partial^2 \zeta}{\partial y^2} \right) = -\frac{\gamma}{\rho} k^2 a S(x, y).$$

Hence

$$\int_{A_f} \mathbf{u} \cdot \mathbf{T} \cdot \mathbf{n} dA = -\frac{\gamma}{\rho} k^2 a \frac{da}{dt} \int S^2 dA. \quad (4.3)$$

The power of traction on the side wall and the bottom wall can be written as

$$\int_{A_w} \mathbf{n} \cdot \mathbf{T} \cdot \mathbf{u} dA = \int_{A_w} \mathbf{n} \cdot (-p\mathbf{1} + 2\mu\mathbf{D}) \cdot \mathbf{u} dA = \int_{A_w} (-p) \mathbf{n} \cdot \mathbf{u} dA + \int_{A_w} \mathbf{n} \cdot 2\mu\mathbf{D} \cdot \mathbf{u} dA. \quad (4.4)$$

Since $\mathbf{n} \cdot \mathbf{u} = 0$ on the side wall and the bottom wall, the power of pressure in (4.4) is zero. For potential flows, we may express the dissipation integral as

$$\int_V 2\mu\mathbf{D} : \mathbf{D} dV = \int_A \mathbf{u} \cdot 2\mu\mathbf{D} \cdot \mathbf{n} dA = \int_{A_f} \mathbf{u} \cdot 2\mu\mathbf{D} \cdot \mathbf{n} dA + \int_{A_w} \mathbf{u} \cdot 2\mu\mathbf{D} \cdot \mathbf{n} dA. \quad (4.5)$$

The integral on A_w will be canceled out by the last term in (4.4) when all the terms are inserted into (2.2). For the integral on A_f we use the expressions in section 3 and find

$$\begin{aligned} \mathbf{u} \cdot 2\mu\mathbf{D} \cdot \mathbf{n} &= -(u_x \tau_{xz} + u_y \tau_{yz} + u_z \tau_{zz}) \\ &= -2\mu \left(\frac{da}{dt} \right)^2 \frac{\coth(kh)}{k} |\nabla_2 S|^2 - 2\mu \left(\frac{da}{dt} \right)^2 k \coth(kh) S^2 \end{aligned}$$

and

$$\int_{A_f} \mathbf{u} \cdot 2\mu\mathbf{D} \cdot \mathbf{n} dA = -4\mu \left(\frac{da}{dt} \right)^2 k \coth(kh) \int S^2 dA. \quad (4.6)$$

The last term in (2.2) is the potential energy and can be written as

$$\begin{aligned} (g - f \cos(\omega t)) \frac{d}{dt} \int_V \rho z dV &= (g - f \cos(\omega t)) \frac{d}{dt} \left\{ \int_A dA \int_{\zeta}^h \rho z dz \right\} \\ &= (g - f \cos(\omega t)) \frac{d}{dt} \left\{ \int_A dA \frac{\rho (h^2 - \zeta^2)}{2} dz \right\} \\ &= -(g - f \cos(\omega t)) \frac{d}{dt} \int \frac{\rho}{2} \zeta^2 dA \\ &= -(g - f \cos(\omega t)) \rho a \frac{da}{dt} \int S^2 dA. \end{aligned} \quad (4.7)$$

Finally using (4.1), (4.2), (4.3) and (4.6) to evaluate (2.2), we get

$$\frac{da}{dt} \left\{ \rho \frac{d^2 a}{dt^2} \frac{\coth(kh)}{k} = -\gamma a k^2 - 4\mu \frac{da}{dt} k \coth(kh) - \rho (g - f \cos(\omega t)) a \right\} \int S^2 dA.$$

Hence

$$\frac{d^2 a}{dt^2} + 4\nu k^2 \frac{da}{dt} + k \tanh(kh) \left[\frac{\gamma}{\rho} k^2 + (g - f \cos(\omega t)) \right] a = 0. \quad (4.8)$$

Equation (4.8) is exactly the same as (3.35), thus the dissipation calculation gives the same results as VCVPF. (4.8) and (3.35) are also in agreement with (4.21) of Kumar & Tuckerman (1994).

5 Stability analysis

The amplitude equations are

$$\ddot{a} + N\nu\dot{a}k^2 + k \tanh(kh) \left[\frac{\gamma}{\rho} k^2 + (g - f \cos(\omega t)) \right] a = 0 \quad (5.1)$$

where

$$N = 2 \text{ (VPF)}, \quad N = 4 \text{ (VCVPF)}. \quad (5.2)$$

In the fourth order RK integration, we may take time difference $\Delta t = \pi/2^{12} = \pi/4096$ for which time at n steps is given by $t = n \times \Delta t$ and periodic time T may be defined as

$$T = \left[\frac{t}{2\pi} \right] \quad (5.3)$$

with Gauss' symbol $[]$. According to Floquet theory, we may represent the solutions of (5.1) in the unstable region as

$$\ln(a(t)) = \sigma t + \beta = \sigma 2\pi T + \beta \quad (5.4)$$

where $\exp(\beta(t)) = b(t)$ is periodic in t but constant in T , and the growth rate σ is positive; $\sigma = 0$ at the marginal state. To check $\exp(\beta(t)) = b(t)$, we may use Fourier series expressed as

$$b(t) = \sum_{n=-\infty}^{\infty} A_n \exp(int) \quad (5.5)$$

where the Fourier coefficient A_{-n} is the complex conjugate of A_n . The coefficient is evaluated as

$$A_m = \frac{1}{2\pi} \int_t^{t+2\pi} b(t) \exp(-imt) dt = \frac{1}{2\pi} \sum_{j=1}^{8192} [b(t_j) \exp(-imt_j) + b(t_{j-1}) \exp(-imt_{j-1})] \frac{\Delta t}{2} \quad (5.6)$$

with the trapezoidal rule; $t_j = t + j \times \Delta t$.

The solution of (5.1) can be written in Floquet form.

$$a(t) = e^{\sigma t} b(t) \quad (5.7)$$

where σ is the growth rate and $b(t)$ is a bounded oscillatory function which is periodic when

$$\sigma = 0 \quad (\text{marginal state}) \quad (5.8)$$

or

$$\sigma > 0 \quad (\text{unstable state}). \quad (5.9)$$

A growth rate curve is given by

$$\sigma = \sigma(k) = \sigma(-k) \quad (5.10)$$

which is an even function of k .

The maximum growth rate is

$$\sigma_m = \max_{k > 0} [\sigma(k)] = \sigma(k_m). \quad (5.11)$$

The flow is stable when $k > k_c$

$$\sigma(k) < 0, \quad k > k_c \quad (5.12)$$

where k_c is called the cut off wave number. This says that short waves are stable.

5.1 Comparison of VPF and VCVPF for periodic waves in a deep liquid

The governing equation (5.1) for the oscillation amplitude in a deep liquid $h \rightarrow \infty$ is

$$\ddot{a} + N\nu\dot{a}k^2 + k \left[\frac{\gamma}{\rho}k^2 + (g - f \cos(\omega t)) \right] a = 0 \quad (5.13)$$

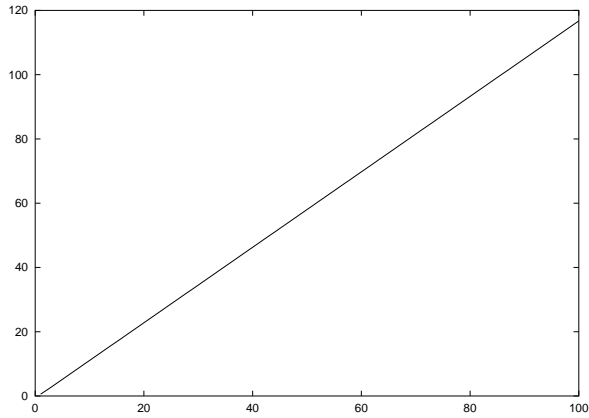
where $N = 2$ (VPF) or $N = 4$ (VCVPF). The main goal of this calculation is to show that for any value of the kinematic viscosity ν , the other parameters being constant, $N = 2$ has a larger maximum growth rate than $N = 4$. Hence, the irrotational theory associated with the direct effects of the viscous normal stress (VPF) on the motion of the waves will give a better description of the effects of viscosity on the waves, than the value $N = 4$ (VCVPF) which has been universally used by researchers in this subject since the study of Kumar & Tuckerman (1994).

Cerda & Tirapegui (1998) considered Faraday's instability in a viscous fluid and found a Mathieu equation based on lubrication theory rather than potential flow. They interpret the irrotational theory leading to $N = 4$ as appropriate to weak dissipation. Our irrotational theories are not restricted to small viscosity, but they do not account for vorticity generated by the no-slip condition on the container side walls or bottom. For periodic disturbances on deep water the irrotational theories are valid for all values of ν .

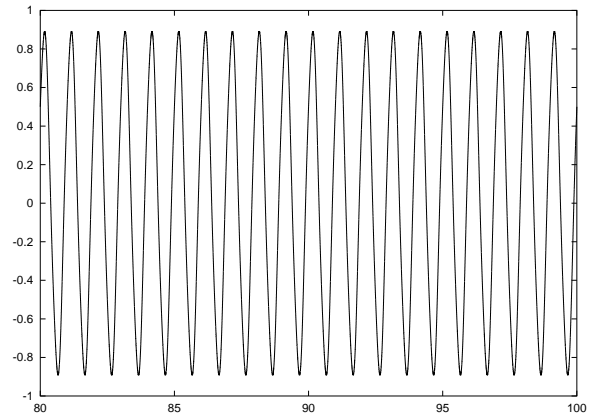
Our results apply to silicon oils with kinematic viscosities ranging from zero to 10 cm²/sec, the density of 0.97 g/cm³ and surface tension of $\gamma = 21$ dyne/cm. The frequency $\omega = 15.87 \times 2\pi$ sec⁻¹ is fixed and $(g, f) = (981, 981)$ cm/sec².

In figure 5.1 and 5.2 we present graphs and tables for the Floquet representation $a = e^{\sigma t}b(t)$ for the stability of Faraday waves on an inviscid and a viscous fluid.

In figure 5.3 we have plotted σ_m vs ν for Faraday waves on an inviscid fluid ($N = 0$) and on a viscous fluid using VPF ($N = 2$) and VCVPF ($N = 4$). These theories are all irrotational. VCVPF is the same as VPF with an added viscous contributions to the pressure. VCVPF gives the same results as the dissipation method as shown here in section 4. Previously, the dissipation theory with $N = 4$, was proposed by Kumar & Tuckerman (1994) from heuristic considerations. In figure 5.4 we plot the critical wave number k_m vs ν . The growth rates and critical wave number are largest for $N = 0$ and are larger for VPF than for VCVPF at each fixed ν .



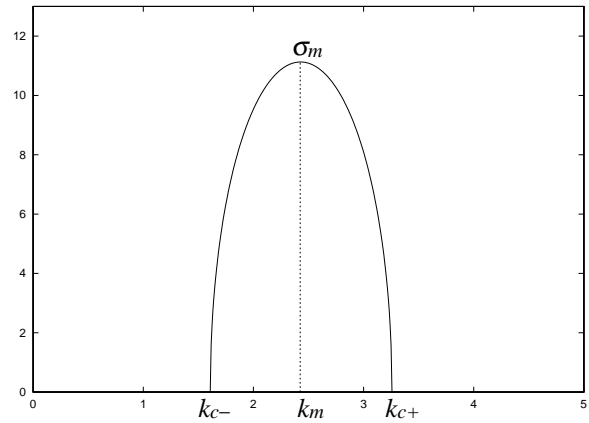
(a) $\ln(a)$ versus $t/(2\pi)$, $k = 1.974 \text{ cm}^{-1}$.



(b) $ae^{-\sigma t}$ versus $t/(2\pi)$, $k = 1.974 \text{ cm}^{-1}$.

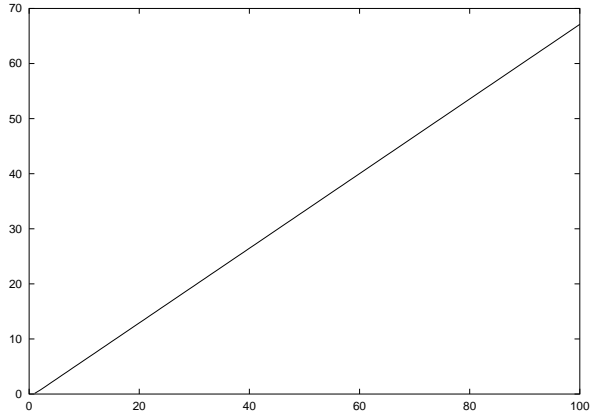
Spectrum of $ae^{-\sigma t}$ for $k = 1.974 \text{ cm}^{-1}$.

n	$\Re\{A_n\}$	$\Im\{A_n\}$
0	-6.9334e-09	0.0000e+00
1	2.6445e-01	-3.4452e-01
2	2.5204e-09	3.7177e-09
3	-1.4703e-02	1.4509e-02
4	3.3942e-10	1.2655e-09
5	2.5412e-04	-2.1465e-04

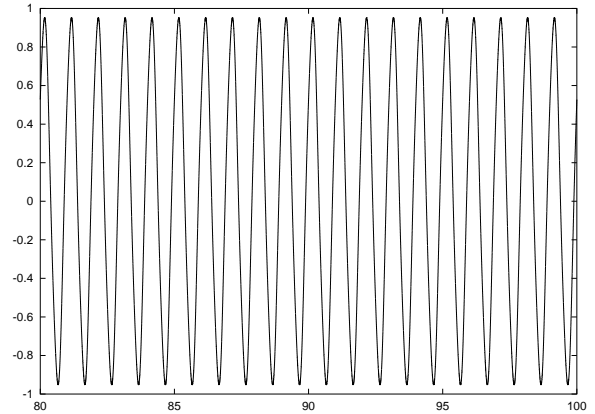


(c) σ versus k .

Figure 5.1: Floquet theory $a = e^{\sigma t}b(t)$ for Faraday waves on an inviscid fluid ($N = 0$); $\rho = 0.97 \text{ g/cm}^3$, $\gamma = 21 \text{ dyne/cm}$, $g = 981 \text{ cm/sec}^2$, $\omega = 2\pi \times 15.87 \text{ sec}^{-1}$, $f = g \text{ cm/sec}^2$. (a) $\ln(a)$ vs $t/(2\pi)$, (b) $ae^{-\sigma t} = b(t) = b(t + 2\pi)$ vs $t/(2\pi)$, (c) $\sigma(N\nu)$ vs k . $\sigma_m = 11.1274 \text{ sec}^{-1}$ at $k_m = 2.4246 \text{ cm}^{-1}$.



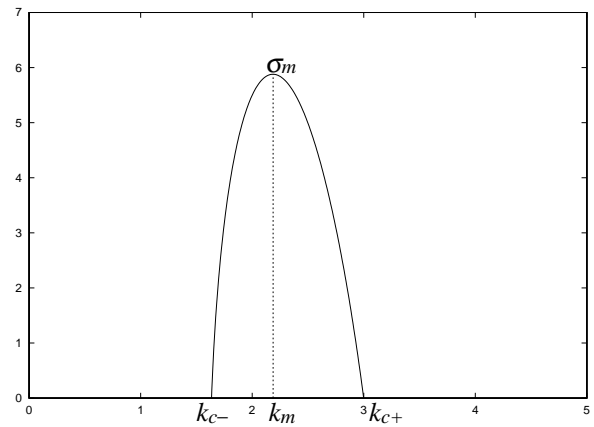
(a) $\ln(a)$ versus $t/(2\pi)$, $k = 1.974 \text{ cm}^{-1}$.



(b) $ae^{-\sigma t}$ versus $t/(2\pi)$, $k = 1.974 \text{ cm}^{-1}$.

Spectrum of $ae^{-\sigma t}$ for $k = 1.974 \text{ cm}^{-1}$.

n	$\Re\{A_n\}$	$\Im\{A_n\}$
0	-7.2599e-09	0.0000e+00
1	2.7907e-01	-3.7011e-01
2	2.6395e-09	3.8242e-09
3	-1.5536e-02	1.5620e-02
4	3.5512e-10	1.3015e-09
5	2.6873e-04	-2.3150e-04



(c) σ versus k .

Figure 5.2: Floquet theory $a = e^{\sigma t}b(t)$ for Faraday waves on a viscous liquid $\nu = 1 \text{ cm}^2/\text{sec}$ with $N = 2$ (VPF); $\rho = 0.97 \text{ g/cm}^3$, $\gamma = 21 \text{ dyne/cm}$, $g = 981 \text{ cm/sec}^2$, $\omega = 2\pi \times 15.87 \text{ sec}^{-1}$, $f = g \text{ cm/sec}^2$. (a) $\ln(a)$ vs $t/(2\pi)$, (b) $ae^{-\sigma t} = b(t) = b(t + 2\pi)$, (c) σ vs k . $\sigma_m = 5.8790 \text{ sec}^{-1}$ at $k_m = 2.1874 \text{ cm}^{-1}$. The dissipation theory with $N = 4$ (VCVPF) is stable $\Re\{\sigma\} < 0$.

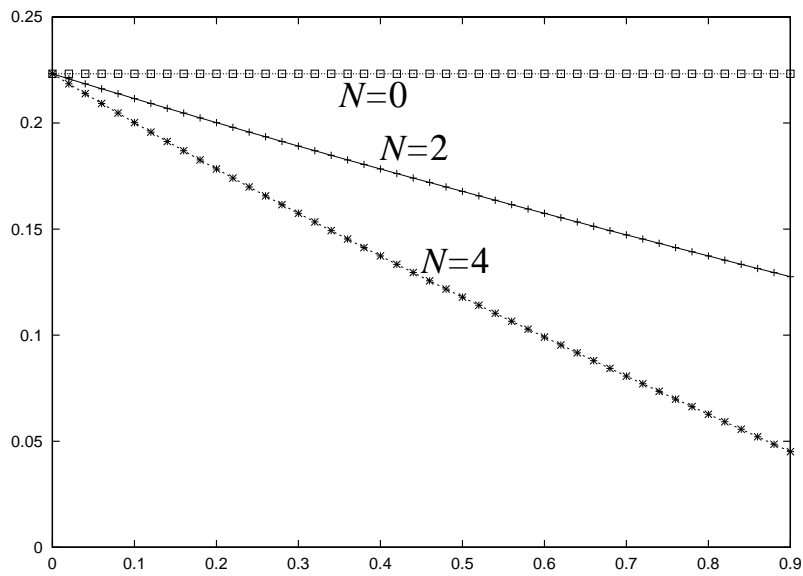


Figure 5.3: σ_m versus ν cm²/sec.

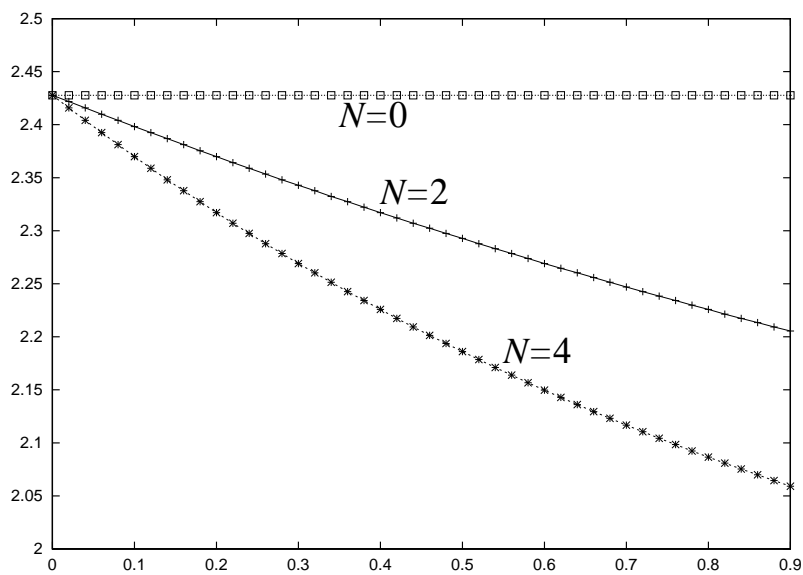


Figure 5.4: k_m versus ν cm²/sec.

5.2 Damped Mathieu equation; Experiments of Benjamin & Ursell

The damped Mathieu equation (5.1) can be transformed into a Mathieu equation through the following change of variables.

Using $a(t) = \hat{a}(t)e^{-N\nu k^2 t/2}$, we have a Mathieu equation:

$$\frac{d^2 \hat{a}}{dt^2} + \left[k \tanh(kh) \left(g + \frac{\gamma}{\rho} k^2 \right) - \left(\frac{N\nu k^2}{2} \right)^2 - fk \tanh(kh) \cos(\omega t) \right] \hat{a} = 0. \quad (5.14)$$

The solution $\hat{a}(t) = e^{\sigma' t} b(t)$ with a temporary growth rate σ' and the periodic function $b(t)$ gives the neutral state when $a(t) = \hat{a}(t)e^{-N\nu k^2 t/2} = e^{\sigma' t} b(t)e^{-N\nu k^2 t/2} = b(t)$, that is, when $\sigma' = N\nu k^2/2$. The effective growth rate is $\sigma = \sigma' - N\nu k^2/2$.

Normalization as $\omega t/2 \rightarrow t$ gives

$$\frac{d^2 \hat{a}}{dt^2} + [p - 2q \cos(2t)] \hat{a} = 0 \quad (5.15)$$

with p and q

$$p = \frac{4}{\omega^2} \left[\left(g + \frac{\gamma}{\rho} k^2 \right) k \tanh(kh) - \left(\frac{N\nu k^2}{2} \right)^2 \right], \quad 2q = \frac{4}{\omega^2} f k \tanh(kh). \quad (5.16)$$

Benjamin & Ursell (1954) studied Faraday waves on an inviscid fluid in a cylindrical container of radius R and height h . For data $[\rho, g, \gamma, h, R, \omega]$ used by them, $\rho = 1 \text{ g/cm}^3$, $g = 981 \text{ cm/sec}^2$, $\gamma = 72.5 \text{ dyn/cm}$, $h = 25.4 \text{ cm}$ (as of infinite depth), $R = 2.7 \text{ cm}$, $\omega = 2\pi \times 15.87 \text{ sec}^{-1}$ and $k = 5.331/R = 1.974 \text{ cm}^{-1}$ and

$$p = \frac{4k}{\omega^2} \left(g + \frac{\gamma}{\rho} k^2 \right), \quad 2q = \frac{4kf}{\omega^2}. \quad (5.17)$$

The stability chart for Mathieu equation in BU (their figure 3) is reproduced in figure 5.5, by picking up their data (q, p) obtained by experiments for the $(2, 1)$ mode of $kR = 5.331 = k_{2,1}R$, for which the value of $k_{m,l}R$ with the radial mode m and the azimuthal mode l gives zero points of the derivative of Bessel functions of the first kind due to the side wall condition of circular cylindrical container. The numbered points in figure 5.5 have the data (q, p) listed in table 5.1, where ω and f are computed with (5.17) for given $[\rho, g, \gamma, k, q, p]$. In table 5.1, listed are the phase function β and the growth rate σ defined by (5.4) for unstable solutions, which are obtained by the RK integration of Mathieu equation (5.15) with (q, p) given by (5.17). In the case of figure 5.5, $b(t)$ is of period π and may be expressed as the Fourier series (5.5).

Using (5.17) for given values of k , we can plot values of p and q in the (q, p) plane as in figure 5.5 and find the cross points at the borders, say (q_1, p_1) and (q_2, p_2) , where the points in $q_1 < q < q_2$ and $p_1 < p < p_2$ are unstable. The two cross points give the cut-off wave number k_{c1} and k_{c2} , and then the maximum growth rate σ_m can be found at the associated wave number k_m in $k_{c1} < k_m < k_{c2}$. In figure 5.6 we plot the growth rate curve σ versus k for the experiment of BU marked by point 3 in figure 5.5 and find that the value $k_{2,1} = 1.974 \text{ cm}^{-1}$ is very close to k_m .

The maximum growth rate parameter σ_m and k_m for the 9 cases in tables 5.1 are listed in 5.2, and we find that k_m deviates from $k_{2,1}$. As shown in table 5.3, the $(1, 4)$ mode with $k_{1,4}$ for No.1-7 cases is included in unstable region. In addition to this, other modes may cause instability for No.8 and 9 cases.

In table 5.4 we list values of the growth rate σ and the phase function β for different values of the viscosity when $N = 2$. We find that Point 5 becomes stable for large value of viscosity.

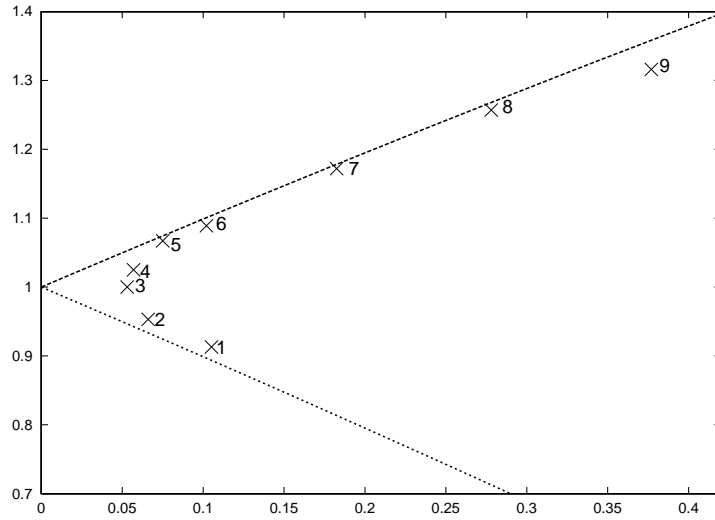


Figure 5.5: p versus q for theoretical stability curve and experimental data of the (2, 1) mode (after Benjamin & Ursell (1954)). The numbered points have the data (q, p) listed in table 5.1.

Table 5.1: Data of q, p, ω, f, β and σ for $\nu = 0$.

No.	q	p	ω	f	β	σ
1	0.1051	0.9130	104.551	290.9270	-6.9315e-01	3.1120e-02
2	0.0660	0.9530	102.333	175.0262	-6.9311e-01	2.3710e-02
3	0.0530	1.000	99.8995	133.9454	-6.9314e-01	2.6491e-02
4	0.0570	1.025	98.6737	140.5410	-6.9313e-01	2.5346e-02
5	0.0750	1.067	96.7122	177.6433	-6.9219e-01	1.5856e-02
6	0.1020	1.089	95.7303	236.7142	-6.9311e-01	2.3172e-02
7	0.1825	1.172	92.2783	393.5386	-6.9310e-01	2.2653e-02
8	0.2780	1.257	89.1037	558.9354	-6.9315e-01	3.6267e-02
9	0.3770	1.316	87.0834	723.9983	-6.9315e-01	7.9969e-02

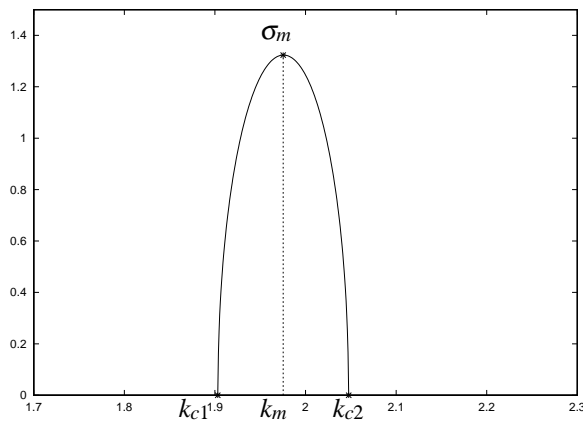


Figure 5.6: σ versus k for point 3, $\nu = 0 \text{ cm}^2/\text{sec}$, $\sigma_m = 0.026495$ at $k_m = 1.9754 \text{ cm}^{-1}$, $k_{c1} = 1.9031 \text{ cm}^{-1}$, $k_{c2} = 2.0476 \text{ cm}^{-1}$.

Table 5.2: Maximum growth rate σ_m is found at $k = k_m$, which is obtained for various values of k by the RK integration of Mathieu equation. Values of $k_m R$ and the cut-off wave number k_c are also computed.

No.	k_m	$k_m R$	σ_m	k_{c1}	k_{c2}
1	2.1044	5.6820	0.055855	1.9474	2.2613
2	2.0444	5.5200	0.034090	1.9476	2.1367
3	1.9694	5.3175	0.026429	1.8993	2.0433
4	1.9444	5.2500	0.028014	1.8669	2.0184
5	1.8894	5.1015	0.035828	1.7935	1.9842
6	1.8644	5.0340	0.048031	1.7371	1.9907
7	1.7744	4.7910	0.081421	1.5665	1.9828
8	1.6994	4.5885	0.11763	1.4070	1.9883
9	1.6594	4.4805	0.15379	1.2861	2.0264

Table 5.3: Wave number $k_{m,l}$ within unstable region and the corresponding growth rate σ . In cases of No.1-7, the (1, 4) mode with $k_{1,4}$ is included in the unstable region $k_{c1} < k < k_{c2}$ shown respectively in table 5.2. In addition to $k_{1,4}$, other modes may cause instability for No.8 and No.9 data.

No.	$k \text{ cm}^{-1}$	σ
1	$k_{1,4} = 1.9695$	$\sigma_{1,4} = 2.8342\text{e-}02$
2	$k_{1,4} = 1.9695$	$\sigma_{1,4} = 2.1715\text{e-}02$
3	$k_{1,4} = 1.9695$	$\sigma_{1,4} = 2.6429\text{e-}02$
4	$k_{1,4} = 1.9695$	$\sigma_{1,4} = 2.6240\text{e-}02$
5	$k_{1,4} = 1.9695$	$\sigma_{1,4} = 1.9213\text{e-}02$
6	$k_{1,4} = 1.9695$	$\sigma_{1,4} = 2.6730\text{e-}02$
7	$k_{1,4} = 1.9695$	$\sigma_{1,4} = 2.8899\text{e-}02$
8	$k_{1,0} = 1.4192$	$\sigma_{1,0} = 3.3493\text{e-}02$
	$k_{1,3} = 1.556$	$\sigma_{1,3} = 1.0233\text{e-}01$
	$k_{1,4} = 1.9695$	$\sigma_{1,4} = 4.2095\text{e-}02$
9	$k_{1,0} = 1.4192$	$\sigma_{1,0} = 1.1758\text{e-}01$
	$k_{1,3} = 1.556$	$\sigma_{1,3} = 1.4769\text{e-}01$
	$k_{1,4} = 1.9695$	$\sigma_{1,4} = 8.2920\text{e-}02$

Table 5.4: Values of the phase function β and growth rate σ defined in (5.4) for viscous fluids with $\epsilon = 4\nu k^2/\omega$ ($N = 2$). Point 5 is unstable for $\nu = 0$ and $\nu = 0.01$ cm²/sec, but stable for large viscosity $\nu = 0.2$ cm²/sec. At the other points, the growth rate σ decreases with increasing ν .

$\nu = 0.01$ cm²/sec

No.	β	σ	ϵ
1	-6.9290e-01	3.0374e-02	1.4915e-03
2	-6.9279e-01	2.29475e-02	1.5238e-03
3	-6.9235e-01	2.5711e-02	1.5609e-03
4	-6.9187e-01	2.4556e-02	1.5803e-03
5	-6.8876e-01	1.5050e-02	1.6124e-03
6	-6.8995e-01	2.2358e-02	1.6289e-03
7	-6.8726e-01	2.1810e-02	1.6899e-03
8	-6.8779e-01	3.5394e-02	1.7501e-03
9	-6.9008e-01	7.9074e-02	1.7907e-03

$\nu = 0.2$ cm²/sec

No.	β	σ	ϵ
1	-6.8822e-01	1.6046e-02	2.9830e-02
2	-6.8668e-01	8.3559e-03	3.0476e-02
3	-6.7763e-01	1.0884e-02	3.1219e-02
4	-6.6839e-01	9.6054e-03	3.1607e-02
5	-6.2691e-01	-1.3444e-06	3.2248e-02
6	-6.3260e-01	7.1299e-03	3.2578e-02
7	-5.8469e-01	6.2595e-03	3.3797e-02
8	-5.9246e-01	1.9260e-02	3.5001e-02
9	-6.3374e-01	6.2351e-02	3.5813e-02

6 Rayleigh-Taylor instability and Faraday waves

This section follows the work of Kumar (2000) who compared wave number selection in Rayleigh-Taylor (RT) instability and Faraday instability on deep and highly viscous liquids. He used the dissipation theory (VCVPF) of Faraday instability with $N = 4$, first proposed by Kumar & Tuckerman (1994). Our main goal is to introduce VPF with $N = 2$ into this comparison. We shall also revise slightly the comparisons made by Kumar (2000) so that a direct comparison of maximum growth rates in the two problems can be made.

Kumar (2000) compared a critical $k_c = k_m$ at $f = f_c$ (where $\sigma(k_m) = 0$, $\sigma < 0$ for $k \neq k_m = k_c$) for Faraday waves with the maximum growth rate of RT waves when the gravitational acceleration is replaced with

$$\bar{a}_c = \frac{\omega}{\pi} \int_{3\pi/2\omega}^{5\pi/2\omega} [f_c \cos(\omega t) - g] dt = \frac{2}{\pi} f_c - g. \quad (6.1)$$

This value of \bar{a}_c is an average upward acceleration in the Faraday problem. He used (6.1) with $N = 4$ in his calculation.

The maximum growth rate for RT instability can be computed from the exact linear theory given by equation (18) in Joseph, Belanger & Beavers (1999) or more easily and with good accuracy by the purely irrotational theory by equation (28) with $\nu = \mu_2/\rho_2$ and g replaced by \bar{a}_c . In this case, their (28) gives

$$\sigma = -k^2\nu \pm \sqrt{k\bar{a}_c - \frac{k^3\gamma}{\rho} + k^4\nu^2}. \quad (6.2)$$

The function $k_m(\bar{a}_c)$ is given by maximizing σ given by (6.2) with respect to k .

$$\frac{d\sigma}{dk} = -2\nu k + \frac{1}{2} \frac{\bar{a}_c - 3\frac{\gamma}{\rho}k^2 + 4k^3\nu^2}{\sqrt{\bar{a}_c k - \frac{\gamma}{\rho}k^3 + k^4\nu^2}} = 0 \quad (6.3)$$

which can be arranged as

$$8\nu^2 k^3 \left(\bar{a}_c + \frac{\gamma}{\rho} k^2 \right) = \left(\bar{a}_c - 3\frac{\gamma}{\rho} k^2 \right)^2. \quad (6.4)$$

This is a fifth order algebraic equation for $k = k_m$. When \bar{a} is large, we have

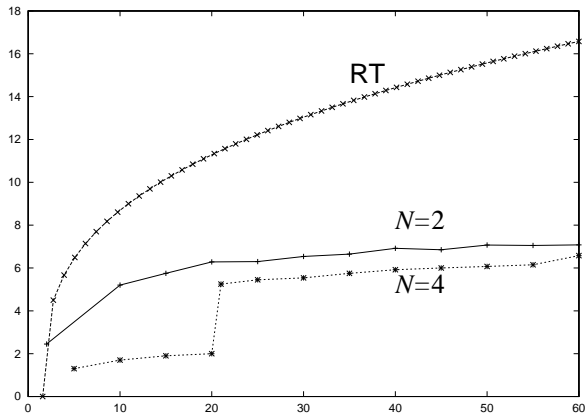
$$8\nu^2 k^3 \bar{a} = (\bar{a})^2. \quad (6.5)$$

Hence

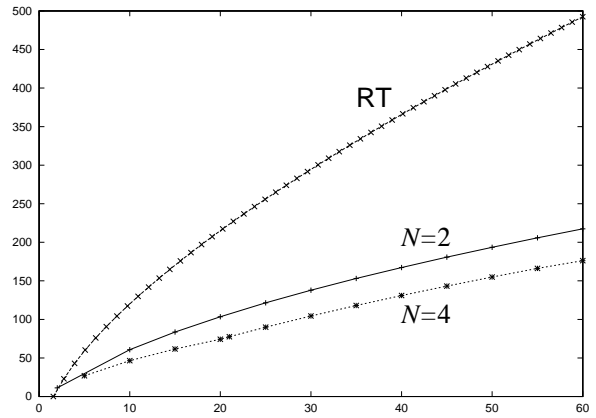
$$k_m = \left(\frac{\bar{a}}{8\nu^2} \right)^{1/3} \quad (6.6)$$

gives the maximum growth rate for large \bar{a} .

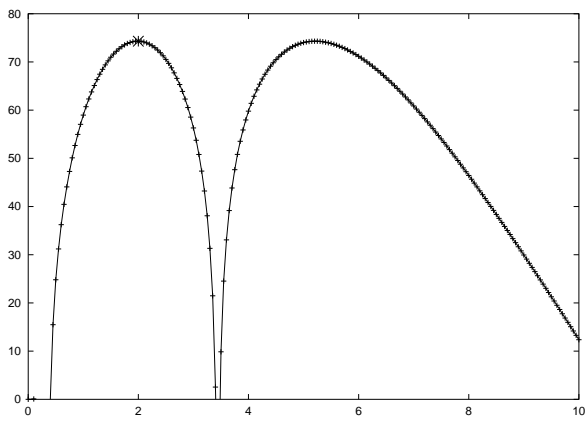
The maximum growth rate $\sigma_m = \sigma(k_m)$ and the wave number $k = k_m$ of maximum growth rate for RT instability and dissipative Faraday waves are compared in figures 6.1, 6.2 and 6.3. These figures show that the dissipative theory with $N = 4$ introduced by Kumar & Tuckerman (1994) and used by Kumar (2000) are more damped than the dissipative potential flow solution VPF with $N = 2$; damped solutions with $\sigma_m < 0$ at small values of f/g are shown in figures 6.2 and 6.3. We can say that the demonstration that damped Faraday waves at large viscosities are driven by the same acceleration mechanism which produce RT waves is better demonstrated by VPF with $N = 2$ than by the dissipative theory which is equivalent to our irrotational VCVPF with $N = 4$.



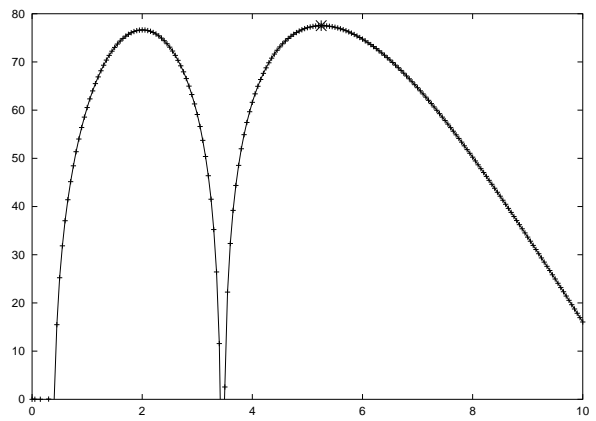
(a) k_m versus f/g .



(b) σ_m versus f/g .

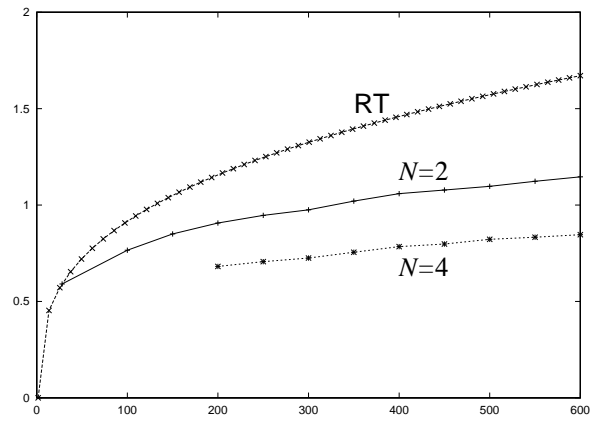


(c) σ versus k for $N = 4$ and $f/g = 20$.

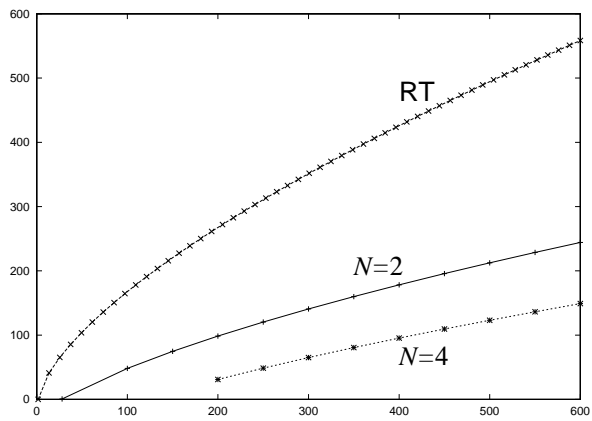


(d) σ versus k for $N = 4$ and $f/g = 21$.

Figure 6.1: (a) k_m versus f/g and (b) σ_m versus f/g , for $\nu = 1 \text{ cm}^2/\text{sec}$. (c), (d) σ versus k for $N = 4$ in a transition region, in which the mark $*$ denotes the maximum growth rate.

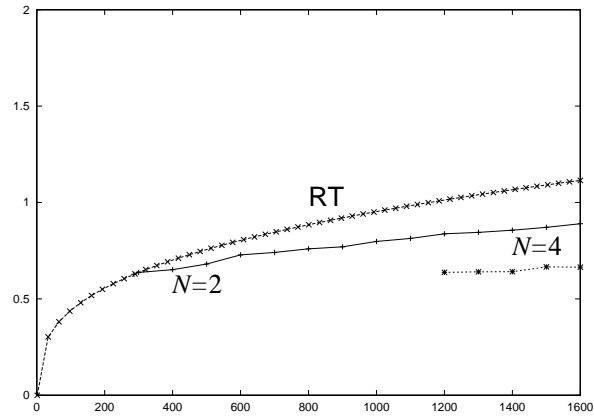


(a) k_m versus f/g for $\nu = 100 \text{ cm}^2/\text{sec}$.

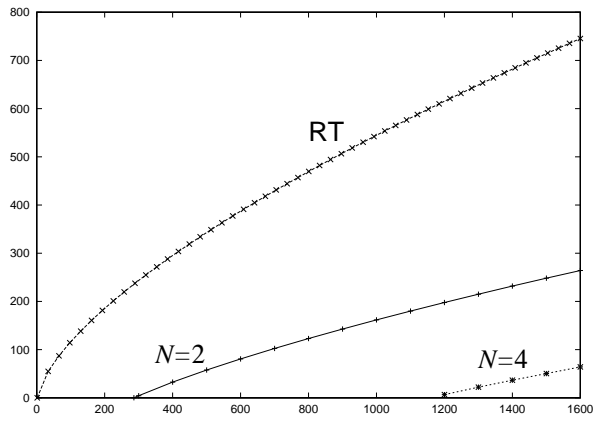


(b) σ_m versus f/g for $\nu = 100 \text{ cm}^2/\text{sec}$.

Figure 6.2: (a) k_m versus f/g and (b) σ_m versus f/g , for $\nu = 100 \text{ cm}^2/\text{sec}$.



(a) k_m versus f/g for $\nu = 300 \text{ cm}^2/\text{sec}$.



(b) σ_m versus f/g for $\nu = 300 \text{ cm}^2/\text{sec}$.

Figure 6.3: (a) k_m versus f/g and (b) σ_m versus f/g , for $\nu = 300 \text{ cm}^2/\text{sec}$. For small values of f/g the potential flow solutions for Faraday waves are stable, $\sigma_m < 0$ but $N = 2$ is less stable and more like RT waves than $N = 4$.

7 Comparison of purely irrotational solutions with exact solutions

Kumar & Tuckerman (1994) presented a linear stability analysis of the interface between two viscous fluids. Starting from the Navier-Stokes equations, they derived the relevant equations describing the hydrodynamic system in the presence of parametric forcing and carried out a Floquet analysis to solve the stability problem. The viscous problem does not reduce to a system of Mathieu equations with a linear damping term, which is traditionally considered to represent the effect of viscosity. The traditional approach ignores the viscous boundary conditions at the interface of two fluids. To determine the effect of neglecting these, they compared their exact viscous fluid results with those derived from the traditional phenomenological approach. They call the exact theory FHS (fully hydrodynamic system). The traditional phenomenological approach is an application of the dissipation method; it is called a model. When applied to an air/liquid system the model is the same as the dissipation method which is the same as our irrotational theory VCVPF with damping proportional to 4ν .

They compared the results of the FHS and of the model to experimental results obtained in a viscous glycerine-water mixture (Edwards & Fauve 1993) in contact with air. They considered the glycerine-water mixture to be a layer of finite height $h = 0.29$ cm, in contact with a layer of air of infinite height. In their figure 3 (our 7.1) they plotted the experimental data for the critical wavelength λ_c and amplitude f_c as a function of forcing frequency. The solid and dashed curves are obtained from the FHS and from the model with finite depth corrections, respectively. They noted, however, that the values for the surface tension γ and the viscosity ν were chosen so as to best fit the FHS to the experimental data. This led to values $\gamma = 67.6 \times 10^{-3}$ N/m and $\nu = 1.02 \times 10^{-4}$ m²/sec, which are in good agreement with the corresponding values given in the literature for the mixture composed of 88% (by weight) glycerol and 12% water, at temperature 23 °C. With these values, both the model and the FHS agree reasonably well with the experimentally measured wavelengths. They noted that "... the experimentally measured amplitudes agree quite well with the FHS over the entire frequency range, and not at all with the model. It is impossible to improve the fit of the critical amplitudes to the model by varying γ and ν ."

The model results shown in the inset for f_c/g in figure 7.1 are for the dissipative approximation VCVPF ($N = 4$).

In figure 7.2 we have compared the exact solution with the irrotational approximation for $N = 4$ and $N = 2$. It is apparent that the fit of the critical amplitudes to the model with $N = 2$ is rather good.

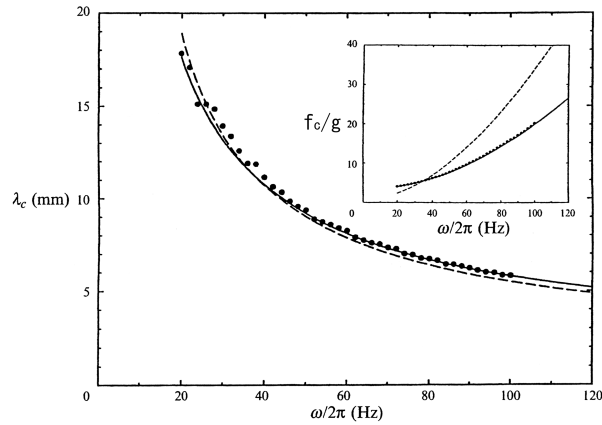


Figure 7.1: Dispersion relation for glycerine-water mixture in contact with air at atmospheric pressure. Fitting the experimental data (Edwards & Fauve 1993) with the results of the FHS (solid lines) leads to $\gamma = 67.6 \times 10^{-3}$ N/m. Inset: Fitting of the experimental data for the stability threshold leads to $\nu = 1.02 \times 10^{-4}$ m²/sec.

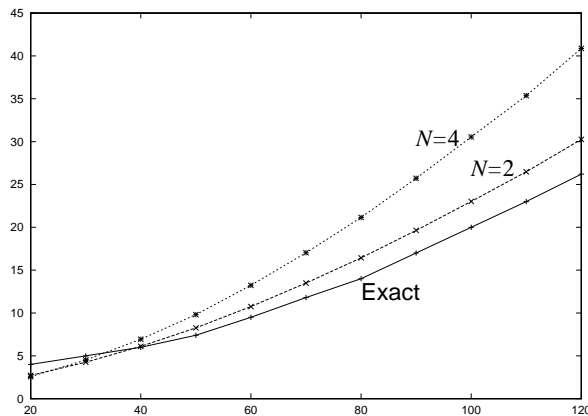


Figure 7.2: f_C/g versus $\omega/(2\pi)$. Based on the data of $\lambda_C = \lambda_C(\omega/(2\pi))$ for their exact solution in figure 7.1 of Kumar & Tuckerman (1994), the critical value f_C/g is estimated for VCVPF and VPF. VPF is closer to the exact solution than VCVPF. $\rho = 1.1848$ g/cm³, $h = 0.29$ cm, $\nu = 1.02$ cm²/sec, $\gamma = 67.6$ dnye/cm.

8 Conclusion

We developed two purely irrotational theories for the effects of viscosity on Faraday waves. In both theories the velocity is computed from the potential and the viscous term in the normal stress balance at the free surface is evaluated on potential flow. In one theory, called VPF, the pressure is given by the Bernoulli equation; it is the same pressure as would be computed for an inviscid fluid. The second irrotational theory, called VCVPF, is the same as the first except for the introduction of an additional pressure generated to remove the unphysical irrotational shear stress from the energy balance. The first theory leads to an amplitude equation with a damping coefficient proportional to 2ν . The second theory leads to the same amplitude equation except that the damping coefficient is proportional 4ν . We show that the VCVPF theory with damping coefficient 4ν is identical to the well known dissipation theory in which no pressure, inviscid or viscous, appears. We show then that the dissipation theory is identical to the damped theory which was introduced by Kumar & Tuckerman (1994) following a heuristic argument. This theory, equivalent to VCVPF, with damping 4ν has been universally regarded as the correct irrotational approximation for viscous damping for small ν . Here, we show that both these ideas are not correct; the VPF theory with damping equal to 2ν is a better approximation and the approximation is not restricted to small viscosities.

References

- Benjamin, T.B. & Ursell, F. 1954. The stability of the plane free surface of a liquid in vertical periodic motion, *Proc. R. Soc. Lond.* **225**, 505-515.
- Cerda, E.A. & Tirapegui, E.L. 1998. Faraday's instability in viscous fluid, *J.Fluid Mech.* **368**, 195-228.
- Dias, F. & Kharif, C. 1999. Nonlinear gravity and capillary-gravity waves. *Annu. Rev. Fluid Mech.* **31**, 301-346.
- Edwards, W.S. & Fauve, S. 1993. Parametrically excited quasicrystalline surface waves, *Phys.Rev. E* **47**, 47R788-R791.
- Funada, T., Wang, J., Joseph, D.D., Tashiro, N., & Sonoda, Y. 2005. Solution of Mathieu's equation by Runge-Kutta integration, <http://www.aem.umn.edu/people/faculty/joseph/ViscousPotentialFlow/>.
- Joseph, D.D., Belanger, J., & Beavers, G.S. 1999. Breakup of a liquid drop suddenly exposed to a high-speed airstream, *Int. J. Multiphase Flow* **25**, 1263-1303.
- Kumar, K. & Tuckerman, L.S. 1994. Parametric instability of the interface between two fluids, *J.Fluid Mech.* **279**, 49-68.
- Kumar, S., 2000. Mechanisms for the Faraday instability in viscous liquids, *Phys.Rev. E* **62**, 1416-1419.
- Landau, L.D. & Lifshitz, E.M. 1987. *Fluid Mechanics* 2nd edition §25, Pergamon.
- Miles, J.W. & Henderson, D.M. 1990. Parametrically forced surface waves. *Annu. Rev. Fluid Mech.* **22**, 143-165.
- Perlin, M. & Schultz, W.W. 2000. Capillary Effects on Surface Waves, *Annual Review of Fluid Mech.* **32**, 241-274.